Direct Measurements of the Interaction between Pyrene and Graphite in Aqueous Media by Single Molecule Force Spectroscopy: Understanding the π−π Interactions

Yiheng Zhang,[†] Chuanjun Liu,[†] Weiqing Shi,[†] Zhiqiang Wang,[†] Liming Dai,[‡] and Xi Zhang*,[†]

Key Lab of Organic Optoelectronics and Molecular Engineering, Department of Chemistry, Tsinghua University, Beijing 100084, P. R. China, and Department of Chemical and Materials Engineering, School of Engineering, University of Dayton, Dayton, Ohio 45469

Pyrene derivatives can absorb onto the surface of carbon nanotubes and graphite particles through π−π interactions to functionalize these inorganic building blocks with organic surface moieties. Using single molecule force spectroscopy, we have demonstrated the first direct measurement of the interaction between pyrene and a graphite surface. In particular, we have connected a pyrene molecule onto an AFM tip via a flexible poly(ethylene glycol) (PEG) chain to ensure the formation of a molecular bridge. The π−π interaction between pyrene and graphite is thus indicated to be ∼55 pN with no hysteresis between the desorption and adhesion forces.

Introduction

The supramolecular approach via noncovalent interactions plays an important role in the surface modification of carbon nanotubes.[1] Having a conjugated all-carbon structure with carbon hexagons arranged in a concentric manner, carbon nanotubes can be conceptually viewed as fully conjugated polyaromatic macromolecules. Recent publications have already established that aromatic molecules, such as pyrene, can anchor onto the graphitic surface of carbon nanotubes noncovalently through π−π interactions in an aqueous medium.[2−5] The interaction of the aromatic system of pyrene with the carbon nanotube is so effective that certain pyrene derivatives tethered onto the nanotube surface have been used as molecular linkages for immobilizing proteins or fabricating layer-by-layer coatings.[2,3] This supramolecular approach based on the π−π interaction can also be applied to flat graphite surfaces.[5]

The π−π interactions (aromatic interactions) are ubiquitous and important in diverse phenomena, including stabilizing DNA and protein structures, packing aromatic molecules in crystals, binding guest moieties to host systems, and supramolecular assembling.[6−10] It has been suggested that π−π interactions consist of electrostatic, hydrophobic, and van der Waals forces.[6−8] Although the π−π interaction has attracted a great deal of interest

from both the theoretical and experimental frontiers, it is still a big challenge to directly measure the π−π interaction at a single molecular level using conventional methods.[6−13] However, the rapid development in atomic force microscopy (AFM) based single molecule force spectroscopy (SMFS) allows for the direct measurement of intermolecular force precisely at a single molecular level.[14−19] In fact, SMFS has been used to detect many intramolecular and intermolecular interactions, including covalent bonding,[20] ligand−receptor pairing,[21] host−guest complexation,[22−24] hydrogen bonding,[25] coordination bonding,[26−28] hydrophobic interaction,[29,30] and charge-transfer interaction.[31,32] Herein, we report results from our recent effort on the use of SMFS to probe the π−π interaction between pyrene and graphite in an aqueous

---

* To whom correspondence should be addressed. Telephone: +86-10-62796283. Fax: +86-10-62771149. E-mail: xi@mail.tsinghua.edu.cn.

† Tsinghua University.

‡ University of Dayton.

(1) Britz, D. A.; Khlobystov, A. N. *Chem. Soc. Rev.* **2006,** *35,* 637.

(2) Chen, R. J.; Zhang, Y.; Wang, D.; Dai, H. *J. Am. Chem. Soc.* **2001,** *123,* 3838.

(3) Paloniemi, H.; Lukkarinen, M.; Aaritalo, T.; Areva, S.; Leiro, J.; Heinonen, M.; Haapakka, K.; Lukkari, J. *Langmuir* **2006,** *22,* 74.

(4) Guldi, D. M.; Rahman, G. M. A.; Zerbetto, F.; Prato, M. *Acc. Chem. Res.* **2005,** *38,* 871.

(5) Ehli, C.; Rahman, G. M. A.; Jux, N.; Balbinot, D.; Guldi, D. M.; Paolucci, F.; Marcaccio, M.; Paolucci, D.; Melle-Franco, M.; Zerbetto, F.; Campidelli, S.; Prato, M. *J. Am. Chem. Soc.* **2006,** *128,* 11222.

(6) Hunter, C. A.; Sanders, J. K. M. *J. Am. Chem. Soc.* **1990,** *112,* 5525.

(7) Hunter, C. A.; Lawson, K. R.; Perkins, J.; Urch, C. *J. Chem. Soc., Perkin Trans. 2* **2001,** 651.

(8) Waters, M. L. *Curr. Opin. Chem. Biol.* **2002,** *6,* 736.

(9) Meyer, E. A.; Castellano, R. K.; Diederich, F. *Angew. Chem., Int. Ed.* **2003,** *42,* 1210.

(10) Hoeben, F. J. M.; Jonkheijm, P.; Meijer, E. W.; Schenning, A. P. H. J. *Chem. Rev.* **2005,** *105,* 1491.

(11) Gonzalez, C.; Lim, E. C. *J. Phys. Chem. A* **2003,** *107,* 10105.

(12) Grimme, S. *J. Comput. Chem.* **2004,** *25,* 1463.

(13) Devic, T.; Yuan, M.; Adams, J.; Fredrickson, D. C.; Lee, S.; Venkataraman, D. *J. Am. Chem. Soc.* **2005,** *127,* 14616.

(14) Janshoff, A.; Neitzert, M.; Oberdörfer, Y.; Fuchs, H. *Angew. Chem., Int. Ed.* **2000,** *39,* 3212.

(15) Hugel, T.; Seitz, M. *Macromol. Rapid Commun.* **2001,** *22,* 989.

(16) Zhang, W.; Zhang, X. *Prog. Polym. Sci.* **2003,** *28,* 1271.

(17) Liu, C.; Shi, W.; Cui, S.; Wang, Z.; Zhang, X. *Curr. Opin. Solid State Mater. Sci.* **2005,** *9,* 140.

(18) Butt, H. J.; Cappella, B.; Kappl, M. *Surf. Sci. Rep.* **2005,** *59,* 1.

(19) Kienberger, F.; Ebner, A.; Gruber, H. J.; Hinterdorfer, P. *Acc. Chem. Res.* **2006,** *39,* 29.

(20) Grandbois, M.; Beyer, M.; Rief, M.; Clausen-Schaumann, H.; Gaub, H. E. *Science* **1999,** *283,* 1727.

(21) Zlatanova, J.; Lindsay, S. M.; Leuba, S. H. *Prog. Biophys. Mol. Biol.* **2000,** *74,* 37.

(22) Schönherr, H.; Beulen, M. W. J.; Bügler, J.; Huskens, J.; van Veggel, F. C. J. M.; Reinhoudt, D. N.; Vancso, G. J. *J. Am. Chem. Soc.* **2000,** *122,* 4963.

(23) Kado, S.; Kimura, K. *J. Am. Chem. Soc.* **2003,** *125,* 4560.

(24) Eckel, R.; Ros, R.; Decker, B.; Mattay, J.; Anselmetti, D. *Angew. Chem., Int. Ed.* **2005,** *44,* 484.

(25) Zou, S.; Schönherr, H.; Vancso, G. J. *J. Am. Chem. Soc.* **2005,** *127,* 11230.

(26) Conti, M.; Falini, G.; Samorì, B. *Angew. Chem., Int. Ed.* **2000,** *39,* 215.

(27) Kudera, M.; Eschbaumer, C.; Gaub, H. E.; Schubert, U. *Adv. Funct. Mater.* **2003,** *13,* 615.

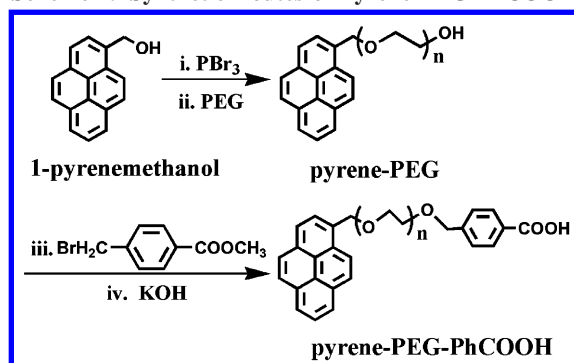(28) Kersey, F.; Yount, W.; Craig, S. *J. Am. Chem. Soc.* **2006,** *128,* 3886.

(29) Cui, S.; Liu, C.; Zhang, W.; Zhang, X.; Wu, C. *Macromolecules* **2003,** *36,* 3779.

(30) Ray, C.; Brown, J. R.; Akhremitchev, B. B. *J. Phys. Chem. B* **2006,** *110,* 17578.

(31) Skulason, H.; Frisbie, C. D. *J. Am. Chem. Soc.* **2002,** *124,* 15125.

(32) Gil, R.; Guillerez, M. G.; Poulin, J. C.; Schulz, E. *Langmuir* **2007,** *23,* 542.

Scheme 1. Synthetic Routes of Pyrene-PEG-PhCOOH

medium. The reported results should underpin our understanding of the formation of supramolecular assemblies through the $\pi-\pi$ interaction.

Experimental Section

Materials and Instruments. 1-Pyrenemethanol was purchased from Sigma-Aldrich. Poly(ethylene glycol) (PEG) was purchased from Acros. The molecular weight of PEG is 6660 g/mol as indicated by matrix-assisted laser desorption ionization time-of-flight (MALDI-TOF) mass spectroscopy, and the polydispersity index of PEG is 1.15 based on gel permeation chromatography (GPC). 3-Amino-propyltriethoxysilane (APTES) was purchased from Fluka. 1-Ethyl-3-(3-dimethyl-aminopropyl) carbodiimide (EDC) was purchased from Shanghai Sanjie Biochemistry Technology. *N*-Hydroxy succinimide (NHS) was purchased from Alfa Aesar. Highly oriented pyrolytic graphite (HOPG) was purchased from Digital Instrument. All solvents were freshly distilled before use.

^{1}H NMR spectra were recorded in CDCl$_3$ solution on a JEOL JNM-ECA300 (300 MHz) spectrometer using tetramethylsilane (TMS) as the internal standard. FT-IR spectra were collected with a Bruker IFS 66V instrument equipped with a deuterated triglycine sulfate (DTGS) detector.

Synthesis. The synthetic route is shown in Scheme 1. All reactions were performed under argon atmosphere.

1-(Bromomethyl) Pyrene. PBr$_3$ (0.045 mL, 0.480 mmol) was added into a solution of 1-pyrenemethanol (0.204 g, 0.879 mmol) in dry CH$_2$Cl$_2$ (15 mL) under stirring. The reaction was carried out at room temperature for 3 h and then quenched by a droplet of water. The reaction mixture was then extracted with CH$_2$Cl$_2$, and the organic layer was dried over Na$_2$SO$_4$. After evaporation of the solvent, the product was purified by silica gel column chromatography eluting with 10:1 petroleum ether/ethyl acetate. Yield: 73%. ^{1}H NMR, δ ppm: 8.39 (d, $J = 9.3$ Hz, 1H, aromatic H), 8.01−8.26 (m, 8H, aromatic H), 5.25 (s, 2H, CH_2Br).

Pyrene-PEG. A mixture of PEG (11.587 g, 1.74 mmol) and NaH (0.201 g, 8.38 mmol) was stirred in dry THF at 40 °C for 2 h. After addition of 1-(bromomethyl) pyrene (0.190 g, 0.644 mmol), the mixture was kept on stirring at 40 °C for 6 h. Thereafter, the solution was concentrated and then precipitated into *n*-hexane under magnetic stirring. The filtered precipitate was purified by silica gel column chromatography eluting with 10:1 CH$_2$Cl$_2$/methanol. Yield: 62%. ^{1}H NMR, δ ppm: 8.39 (d, $J = 9.3$ Hz, 1H, aromatic H), 8.00−8.22 (m, 8H, aromatic H), 5.28 (s, 2H, pyrene−CH_2), 3.35−3.90 (m, ~600H, CH$_2$−CH_2O).

Pyrene-PEG-PhCOOCH$_3$. Methyl 4-(bromomethyl)benzoate was synthesized according to the published procedure.[33] NaH (0.204 g, 8.50 mmol) was added to 1.531 g (0.225 mmol) of pyrene-PEG dissolved in THF (30 mL). After the solution was stirred for 1 h at 40 °C, methyl 4-(bromomethyl)benzoate (0.174 g, 0.758 mmol) was added and the solution was kept on stirring for 10 h at 40 °C. The solvent was concentrated, and then the solution was precipitated into *n*-hexane. The filtered precipitate was purified by silica gel

column chromatography eluting with 10:1 CH$_2$Cl$_2$/methanol. Yield: 52%. ^{1}H NMR, δ ppm: 8.40 (d, $J = 9.3$ Hz, 1H, aromatic H), 7.97−8.22 (m, 10H, aromatic H), 7.41 (d, $J = 8.3$ Hz, 2H, phenyl H), 5.28 (s, 2H, pyrene−CH_2), 4.62 (s, 2H, phenyl−CH_2), 3.90 (s, 3H, COOCH_3), 3.35−3.90 (m, ~670H, CH$_2$−CH_2O).

Pyrene-PEG-PhCOOH. Pyrene-PEG-PhCOOCH$_3$ (0.824 g, 0.118 mmol) was refluxed in mixed solution of 20 mL of 1 M KOH aqueous solution and 10 mL of THF for 9 h. After cooling to room temperature, THF was evaporated and the residue was acidified with 1 M HCl until pH 7. The solution was extracted with CH$_2$Cl$_2$, and then the organic layer was dried over Na$_2$SO$_4$. Evaporation of the solvent in vacuum gave a yellow powder of the product (0.717 g, 0.102 mmol). Yield: 87%. ^{1}H NMR, δ ppm: 8.40 (d, $J = 9.3$ Hz, 1H, aromatic H), 7.97−8.22 (m, 10H, aromatic H), 7.41 (d, $J = 7.9$ Hz, 2H, phenyl H), 5.29 (s, 2H, pyrene−CH_2), 4.62 (s, 2H, phenyl−CH_2), 3.35−3.90 (m, ~670H, CH$_2$−CH_2O). IR: ν (cm^{-1}) 3039, 2881, 2740, 2694, 2237, 1718, 1612, 1466, 1414, 1358, 1344, 1281, 1240, 1147, 1061, 960. MALDI-TOF MS: 6999 (calculated: 7026).

PEG-PhCOOH. The synthetic procedure for preparing PEG-PhCOOH is the same with steps iii and iv in Scheme 1, using PEG as the starting material. ^{1}H NMR, δ ppm: 8.00 (d, $J = 8.0$ Hz, 2H, phenyl H), 7.40 (d, 2H, phenyl H), 4.62 (s, 2H, phenyl−CH_2), 3.35−3.90 (m, ~600H, CH$_2$CH$_2$O).

AFM Tip Modification. After being immersed in CHCl$_3$ for 10 min to remove any possible contamination, the AFM tips were silanized in a solution of APTES in dry toluene (0.05% v/v) for 5 min at room temperature. Thereafter, the silanized AFM tips were washed with CH$_2$Cl$_2$ and methanol several times, followed by drying against filter paper every time after washing. Finally, the clean silanized tips were oven-dried at 60 °C for 1 h and subsequently immersed into a solution of pyrene-PEG-PhCOOH in dry dimethyl sulfoxide (DMSO, ~0.06 mM) for 5 min in the presence of EDC (~0.1 mM) and NHS (~0.05 mM) to allow for the covalent attachment of pyrene-PEG-PhCOOH onto the silanized tip surface.[27] The pyrene-attached AFM tips thus prepared were then washed several times with ethanol and water, dried by touching against filter paper, and used for the force measurements immediately.

SMFS. SMFS measurements were carried out on a Molecular Force Probe 3D instrument (Asylum Research, Santa Barbara, CA). V-shaped Si$_3$N$_4$ cantilevers from Veeco (Santa Barbara, CA) were used. The spring constants of the cantilevers were in the range of 0.010−0.030 N/m according to the measurement of their thermal fluctuation.[34]

To directly measure the interaction between pyrene and graphite, we connected a pyrene molecule onto an AFM tip through a flexible PEG chain end-functionalized with a carboxyl group (i.e., PEG-PhCOOH). While the carboxyl end group was attached to the AFM tip, the other end of the PEG-PhCOOH chain was covalently bonded with a pyrene molecule. The use of PEG as a flexible spacer provides a means for differentiating the force signals based on the extension length and thereby for avoiding the disturbance of the nonspecific interaction between the AFM tip and substrate. The polymer used in this study has a PEG molecular weight of 6660 g/mol with a polydispersity of 1.15 and therefore has a contour length of ~56 nm.

The force measurements were carried out on freshly cleaved HOPG substrates in an aqueous solution containing 0.05% (v/v) polyoxy-ethylene sorbitan monolaurate (Tween 20) or phosphate buffered saline (PBS) at room temperature (~25 °C). Tween 20 was added at a concentration of 0.05% (v/v) to minimize the nonspecific interactions between the tip and the substrate in pure water.[35] (For a comparison of the force measurements in pure water and aqueous media, see the Supporting Information.) Prior to the force measurement, a droplet of the aqueous solution, acting as a buffer, was injected between the substrate and the cantilever holder. Both the substrate and the cantilever were then immersed into the measuring liquid. By controlling the movement of the piezo tube, the AFM tip tethered with pyrene was carefully brought into contact with the

(33) Zhang, X.; Xu, H. P.; Dong, Z. Y.; Wang, Y. P.; Liu, J. Q.; Shen, J. C. *J. Am. Chem. Soc.* **2004**, *126*, 10556.

(34) Butt, H. J.; Jaschke, M. *Nanotechnology* **1995**, *6*, 1.
(35) Krautbauer, R.; Rief, M.; Gaub, H. E. *Nano Lett.* **2003**, *3*, 493.
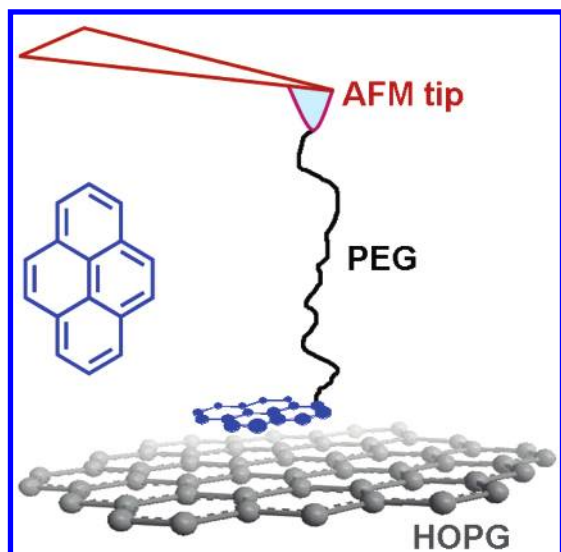
Figure 1. Schematic setup for measuring the $\pi-\pi$ interaction between pyrene and graphite in aqueous medium by SMFS.
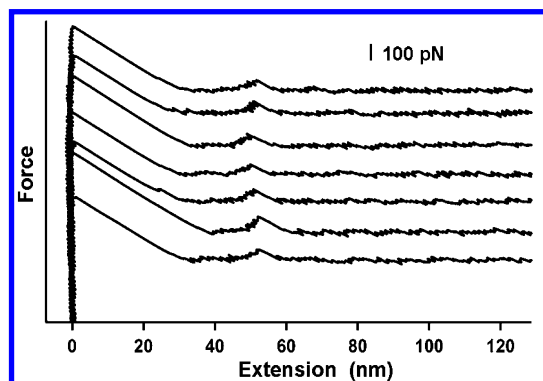

Figure 2. Force curves of pyrene modified tips desorbed from graphite substrate in aqueous medium under a retraction velocity of 500 nm/s (room temperature).

HOPG substrate, as schematically shown in Figure 1. The pyrene-tethered AFM tip was left there without disturbance for ~2 s under a contact force of ~200 pN to ensure that the pyrene group absorbs on the graphite substrate. Upon retracting the AFM tip from the graphite substrate, the AFM cantilever was deflected and the PEG "bridge" was stretched. Meanwhile, a deflection−displacement curve was recorded to produce a force−extension curve (or force curve in short).

Results and Discussion

Single molecular ruptures were observed from the SMFS measurements on the interactions between pyrene and graphite. Figure 2 shows some typical force−extension curves acquired in an aqueous solution at a retraction velocity of 500 nm/s. The initial sharp peak for each of the force curves corresponds to the nonspecific adhesion force between the tip and graphite. This peak is subsequently followed by a small force signal at ~50 nm of the extension length, around which the force increases first with the extension of the polymer chain and then rapidly drops to zero after the rupture point is reached. The extension length of ~50 nm at which the force signal appears is significant evidence of a single molecular rupture event, as this value agrees well with the contour length of the PEG chain (~56 nm) used. Thus, the single molecular rupture event is clearly evident by these force curves with one single force peak (not considering the adhesion force peak); its height indicates that a pull-out force of ~55 pN is required to separate the adsorbed pyrene from the graphite substrate.
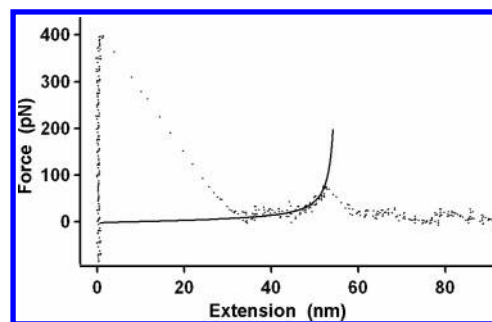

Figure 3. A typical M-FJC model fit curve (solid line). The fitting parameters are $l_k = 0.81 \pm 0.10$ nm and $K_s = 150 \pm 10$ N/m, which are in accordance with that of a single PEG chain.

To further confirm that the observed force signals at the extension length of ~50 nm indeed originate from the single molecule rupture events, we have also used the modified freely jointed chain (M-FJC) model to approximately estimate the elasticity of the single polymer chains.[15,16,36] The M-FJC model treats the polymer as a chain of statistically independent Kuhn segments (segment elasticity, K_s) with a length of l_k (Kuhn length), and the segments can be deformed under external stress. This model is based on the extended Langevin function:

$$x(F) = \left[\coth\left(\frac{Fl_k}{k_BT}\right) - \frac{k_BT}{Fl_k}\right]\left(L_c + \frac{nF}{K_s}\right)$$

where x represents the extension of a polymer chain (end-to-end distance; in our SMFS experiments, therefore, x is the distance between the AFM tip and substrate surface), F is the applied force upon an individual polymer chain, L_c is the contour length of the polymer chain, l_k is the length of the statistically independent segment (i.e., Kuhn length), n is the number of segments being stretched (which is equal to L_c/l_k), k_B is the Boltzmann constant, and T is the Kelvin temperature. The deformation of stretching segments is characterized by K_s. The elasticity of a modified FJC chain is dominated by either the entropic contribution in the low-force region or the enthalpy in the high-force region. We used Igor Pro software (version 5.04B) to carry out the M-FJC fitting. It was found that these force curves can be fitted well by the parameters $l_k = 0.81 \pm 0.10$ nm and $K_s = 150 \pm 10$ N/m, as exemplified by one of the typical fitting curves shown in Figure 3. The good consistency between these fitting parameters with small standard deviations and the corresponding data reported for a single PEG chain[37] strongly indicates that the observed force curves before the rupture points arise from the single chain stretching of PEG. Consequently, the small force peaks observed at the extension length of ~50 nm reflect, once again, the single molecular rupture events. Certainly, it is also possible to observe force profiles when two or more molecules are attached in some cases. If force curves have two single peaks or one peak but two apexes, they may originate from two pyrene molecules detached from the substrate. However, these force profiles show a clear disagreement with the criteria of single chain manipulation.

The single molecular rupture events observed above should correspond to the rupture of the pyrene−graphite binding, indicating the strength of the $\pi-\pi$ interaction between the pyrene molecule and the graphite surface. Figure 4 shows the histogram of the rupture forces between pyrene and graphite at a loading rate of 4.0 ± 0.4 nN/s. The loading rate was derived from the slope of the force−time curve with ~10 data points just before

(36) Li, H.; Liu, B.; Zhang, X.; Gao, C.; Shen, J.; Zou, G. *Langmuir* **1999**, *15*, 2120.

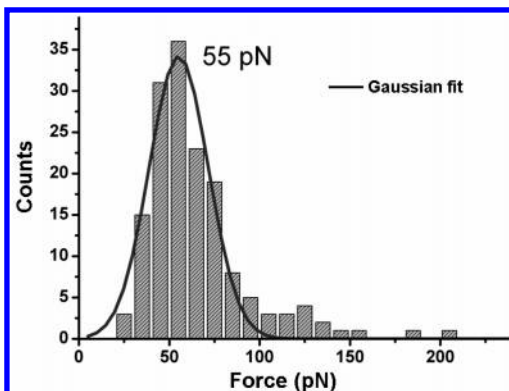(37) Oesterhelt, F.; Rief, M.; Gaub, H. *New J. Phys.* **1999**, *1*, 6.1.

Figure 4. Histogram of the rupture force of the interaction between pyrene and graphite at a loading rate of 4.0 nN/s. The most probable rupture force is 55 pN (with a width of distribution of 16 pN).
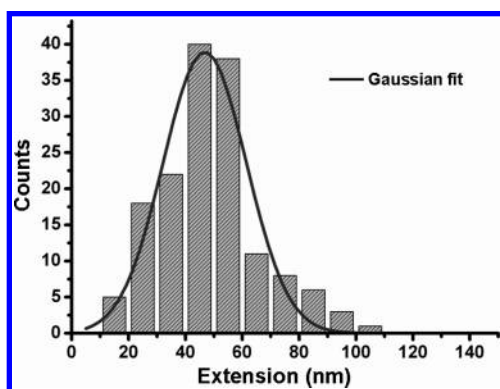

Figure 5. Distribution of the rupture extension of force curves at a loading rate of 4.0 nN/s.

the rupture point being chosen to produce the slope by a linear least-squares fit. As can be seen in Figure 4, the most probable rupture force was found to be ∼55 pN by Gaussian fitting (width of distribution: 16 pN). Figure 5 shows the distribution of the rupture extension obtained from the force curves at a loading rate of 4.0 ± 0.4 nN/s. The different extension values seen in Figure 5 can be attributed to the polydispersity of the PEG chains and/or the different anchoring locations of the PEG spacers on the AFM tip. The most probable rupture extension was found to be 47 nm by Gaussian fitting (width of distribution: 15 nm), which is consistent with the PEG contour length of ∼56 nm.

It is important to compare our force results in a single molecular level to the binding energy, although the exact rupture distance depending on the precise profile of the interaction potential along the pathway is still not known. Considering the distance of the unbinding process of pyrene from the substrate is ∼8 Å, the rupture force multiplied by the distance gives an estimation of the unbinding energy of ∼26 kJ/mol. The binding energy of pyrene on the surface of a carbon nanotube and graphite was calculated to be ∼0.42 eV (∼40.8 kJ/mol) from *ab initio* calculations,[38] but this value varies among different computational methods.[5,38] In general, our result is in the same order of magnitude with these values.

Is there any rate dependence of the interaction between pyrene and graphite measured by SMFS? To address this issue, we performed the SMFS experiment with different retraction velocities ranging from 300 to 4000 nm/s. The relationship between the most probable rupture force and the corresponding loading rate in a logarithmical scale is given in Figure 6, which
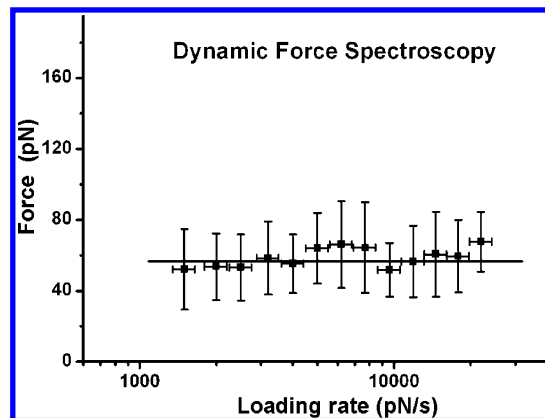
(38) Tournus, F.; Latil, S.; Heggie, M. I.; Charlier, J. C. *Phys. Rev. B* **2005**, *72*, 075431.

Figure 6. Plot of the most probable rupture force between pyrene and graphite as a function of the corresponding loading rate in a logarithmical scale.

indicates that there is no loading rate dependence. This is reasonable given that the time scale for the AFM measurement (in the range of milliseconds) is much slower than that for the fast interaction of pyrene and graphite (less than 1 ns).[5] This result also implies that our experiments were carried out under a quasi-equilibrium condition. Therefore, the observed rupture force should equal the adhesion force between pyrene and graphite.

It is worth it to point out here that optimization of the experimental conditions is crucial for successful single-molecule measurements. In this regard, we modified the AFM tips using a very low concentration of pyrene-PEG-PhCOOH (10^{-5} mol/L) and a short modification time to minimize the surface density of the tethered PEG chains. To make the force measurements more convincing, we have also performed the following control experiments. First, we checked possible effect(s) of solute molecules in the measuring liquid by carrying out the force measurements in an aqueous solution containing phosphate buffered saline (PBS, pH 7.4, 1 tablet/200 mL H_2O; for details, see the Supporting Information). Similar to the case of the addition of Tween 20, the nonspecific force signals can also be reduced upon addition of PBS in water, and the most probable rupture force was measured to be 47 ± 16 pN at 4.0 nN/s in the PBS aqueous solution. If we consider an error of ∼10 pN for the AFM measurements, this value of 47 ± 16 pN is similar to the most probable rupture force measured in the Tween 20 aqueous solution (55 ± 15 pN at 4.0 nN/s). Furthermore, the dynamic force spectroscopy measurements (force versus loading rate plot) also do not show any loading-rate dependence, as is the case with the Tween 20 aqueous solution. These results suggest that the nature of the solutes (Tween 20 or PBS) added to minimize the nonspecific forces shows no obvious effect on the measured specific interaction between pyrene and graphite. Second, we synthesized PEG-PhCOOH for modifying the AFM tip using the same procedure albeit without pyrene. SMFS experiments carried out under the same condition showed force curves with no repeatable single molecule rupture events, except for some nonspecific adhesion peaks.

Conclusions

In summary, we have demonstrated for the first time a direct measurement of the interaction between pyrene and graphite in an aqueous medium by SMFS under quasi-equilibrium conditions. Our results indicate that the $\pi-\pi$ interaction between a pyrene molecule and graphite is ∼55 pN with no loading rate dependence.

Single molecular rupture events have been clearly observed, which were further confirmed by the force curve fitting using the M-FJC model. The fact that all the force measurements were carried out in aqueous solutions could make the results obtained in this study particularly useful for understanding $\pi-\pi$ interaction induced supramolecular assembling in biological systems. Furthermore, the reliable single molecular interaction measurements demonstrated in this study should make the SMFS technique attractive for investigating various other $\pi-\pi$ interaction systems.

Supporting Information Available: Comparison of the force curves in pure water and aqueous medium, and histograms of rupture forces at different loading rates. This material is available free of charge via the Internet at http://pubs.acs.org.

LA700876D